

Bell states in a resonant quantum waveguide network

Gursoy B. Akguc, Linda E. Reichl, Anil Shaji, and Michael G. Snyder

Center for Studies in Statistical Mechanics and Complex Systems, The University of Texas at Austin, Austin, Texas 78712, USA

(Received 14 November 2003; published 5 April 2004)

We show that a network of ballistic electron waveguides can generate entangled Bell-like states from separable states when it is resonant. The network we study is grouped into individual qudits ($d=4$) made up of pairs of waveguides. Rotation gates in the network produce coherent superpositions of qudit states. A Coulomb gate entangles the qudits. We construct a unitary matrix which characterizes the network dynamics and allows a more systematic study of that dynamics.

DOI: 10.1103/PhysRevA.69.042303

PACS number(s): 03.67.Mn, 03.65.Ud, 73.23.Ad

I. INTRODUCTION

There is a great interest in developing quantum networks capable of processing quantum information and performing quantum computations. Ionicioiu *et al.* [1] have suggested use of solid-state electron waveguides for this purpose, with two parallel electron waveguides representing a two-state qubit. One waveguide represents the state $|1\rangle$ and the other the state $|0\rangle$. A single electron can be distributed between the waveguides, thus representing superpositions of the states $|1\rangle$ and $|0\rangle$. Couplings between the two waveguides forming a qubit and couplings between qubits form the unitary transformations necessary to do simple quantum computations. In an ideal network of this type, an electron injected into one of the waveguides will travel through a static network of gates and emerge on the other side of the network in the desired computed state. However, in real waveguide networks there is a finite probability that an electron injected from one side will reflect from a gate and emerge from the network on the input side. The end result of the computation finds an electron in not one of two states, but one of four. The directionality of electron flow in the waveguide requires that we generalize our analysis of waveguide qubits to waveguide *qudits* ($d=4$) [2–4] in order to better understand the dynamics of the system and ultimately the dynamics of specific computations. [A qudit is a d -dimensional quantum state [2–4]. Our network is composed of qudits with $d=4$ which we subsequently call *quqits*. Note that a qubit is a quantum binary digit (see Ref. [5] for the origin of *bit*) and a quqit is a quantum quaternary digit.]

In this paper we study the simplest type of quantum network using solid-state electron waveguides which contains the unitary transformations necessary for quantum computation. We focus on the waveguide network first proposed by Ionicioiu *et al.* [6,7] which will allow us to inject electrons on one side and emit electrons in entangled Bell states on the other side. The significance of producing Bell states starting from a separable state is that it shows that both coherent superpositions and entanglement of qubits can be successfully achieved in networks of quantum waveguides. Only after establishing this basic requirement can one proceed to consider issues such as scalability and robustness of a quantum computational algorithm implemented using the waveguides.

For concreteness, we will assume that the electron waveguide network is formed at a GaAs/Al_xGa_{1-x}As interface, although there are other ways to realize such a device. In a typical GaAs/Al_xGa_{1-x}As based system [8–10] a two-dimensional electron gas (2DEG) is located ≈ 500 Å below the surface of the GaAs/Al_xGa_{1-x}As heterostructure. Leads and cavities can be formed at the interface by depositing metal gates on the surface of the heterostructure and applying a negative voltage to the metal gates. This depletes the electrons from regions of the electron gas below the gates and confines the electrons to the leads and cavities. The electron gas is two-dimensional because only the lowest energy state in the direction perpendicular to the plane of the interface is occupied. At temperatures of $T \sim 0.1$ – 2.0 K, scattering events due to electron-phonon interactions have a mean free path, $L_{ph} \sim 30$ μm [11], and phase decoherence due to electron-electron scattering becomes negligible [11]. Thus, the electron waves can travel through the leads and cavities ballistically.

We begin, in Sec. II, by introducing the states that describe the state of the network, the scattering matrices (S matrices) that represent the dynamics of the gates, and transfer matrix which governs the flow of electrons across the network. In Sec. III, we discuss the geometry of the rotation gates and their transmission properties. In Sec. IV, we introduce a simple gate which, using the Coulomb interaction between electrons, can entangle the electrons on different quqits. Having established the electron dynamics in the gates, in Sec. V we obtain some stationary states of the quantum network and show that under resonance conditions Bell states are possible. We also obtain a unitary matrix which can be used to characterize the dynamics of the network. In Sec. VI, we use the unitary matrix to show that, as the degree of reflection increases, the eigenvalues of the unitary matrix begin to display increasing level repulsion, a signature of broken symmetry. We also show that this is accompanied with a sharp drop in the “fidelity” of the network output. Finally in Sec. VII, we make some concluding remarks.

II. QUANTUM NETWORK

We shall consider the waveguide network shown in Fig. 1. It consists of four leads, the top two leads together form quqit A and the bottom two quqit B . An electron can flow

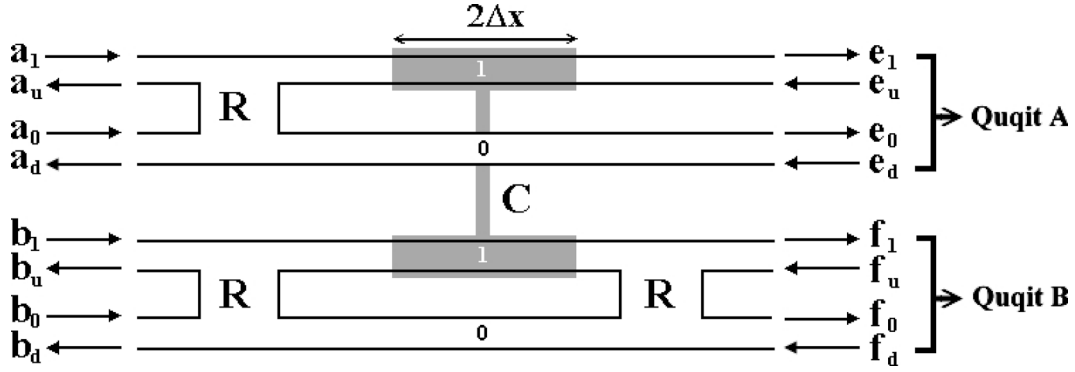


FIG. 1. The quantum network. R locates the rotation gates and C locates the Coulomb gate which couples the state $|1\rangle$ on the two quqits.

freely through its own quqit, but it cannot leave that quqit. Therefore, electrons on different quqits are distinguishable. Within a quqit the leads are coupled by “rotation” gates and the quqits themselves are coupled by a Coulomb interaction window (a Coulomb gate). Rotation gates act on incident states within a quqit and create exit states which are superpositions of states of the quqit. This type of rotation of the state of the system is required for the implementation of quantum logical structures. In systems of qubits some examples of such gates include the Hadamard gate and the square root of the NOT gate [12] which we denote as the $\sqrt{\text{NOT}}$ gate. We will show how these gates can be implemented in quqit systems.

Several proposals for the construction of rotation gates and other gate elements in networks of electron wave guides are discussed in Refs. [13–16]. For simplicity, we will assume that the walls of leads and rotation gates are infinitely hard and the leads are very long compared to the length of the gates. In the leads, the electrons propagate along the x direction and set up standing waves along the y direction. For GaAs/ $\text{Al}_x\text{Ga}_{1-x}\text{As}$ based devices, the Fermi energy of the two-dimensional electron gas in the waveguide is $E_f = \pi n_e \hbar^2 / m$, where \hbar is Planck’s constant, n_e is the density of electrons, and m is the effective mass of the electrons. Both n_e and m depend on the materials used to construct the 2DEG. For GaAs, the electron effective mass is $m = 0.067m_e$, where m_e is the mass of a free electron. When the electron density is $n_e = 1.0 \times 10^{12} \text{ cm}^{-2}$, for example, the Fermi energy is $E_f = 0.048 \text{ eV}$ and can be varied by varying the electron density.

The electron energies in each of the four leads have the form

$$E = \frac{\hbar^2}{2m} \left[k_n^2 + \left(\frac{n\pi}{w} \right)^2 \right], \quad (1)$$

where w is the width of each of the leads and index $n = 1, 2, \dots, \infty$ denotes the number of antinodes associated with the transverse parts of the electron states in the leads. The electron states in the leads take the form

$$\Phi_{k_n}(x, y) = \chi_{k_n}(x) \sqrt{\frac{2}{w}} \sin\left(\frac{n\pi y}{w}\right), \quad (2)$$

where n is the quantum number associated with the transverse modes in the leads and $\chi_{k_n}(x)$ is the longitudinal part of the wave function in the leads.

We will choose the Fermi energy of electrons in the waveguide network so that electron wave propagation can only occur in the first channel, $n=1$, in each of the leads. To simplify notation, we will work in terms of dimensionless scaled quantities. We choose our unit of energy to be $E_0 = \hbar^2 / 2mw_0^2 = 0.000355 \text{ eV}$ and our unit of length to be $w_0 = 400 \text{ \AA}$. The scaled electron wave vector in the first channel is then $\kappa = k_1 w_0$. Let us write the scaled Fermi energy as $E = E_f / E_0$. We will assume all four leads have a width $w = 160 \text{ \AA}$. Then electron propagation can only occur if $(\pi/0.4)^2 \leq E \leq (2\pi/0.4)^2$ or $61.7 \leq E \leq 246.8$. The scaled Fermi energy in the first channel can be written as $E = \kappa^2 + 61.7$.

We will treat the electron flow in the waveguide network as a scattering system and determine Fermi energies at which we might be able to generate Bell states. We will keep our notation and interpretation of the dynamics in the waveguide network as close as possible to that used in the quantum computing literature [12]. The waveguide network in Fig. 1 has two quqits which we denote A and B . We denote the states for electrons in quqit A which travel to the right (left) in the upper and lower leads as $|1\rangle_A$ and $|0\rangle_A$ ($|u\rangle_A$ and $|d\rangle_A$), respectively. Similarly, we denote the states for electrons in quqit B which travel to the right (left) in the upper and lower leads of quqit B as $|1\rangle_B$ and $|0\rangle_B$ ($|u\rangle_B$ and $|d\rangle_B$), respectively.

For simplicity, we will always assume that the electrons are injected into the network from the left. Because of the gates, the electron probability amplitudes in the various segments of each quqit will vary as the electrons traverse the network from left to right. As we will show below, we can relate the probability amplitudes for the allowed states on the left to those on the right. Our notation for these probability amplitudes is indicated in Fig. 1. The probability amplitudes of *right flowing* electrons will have subscripts 1 and 0 for the upper and lower leads, respectively, for each quqit. The probability amplitudes of *left flowing* electrons will have sub-

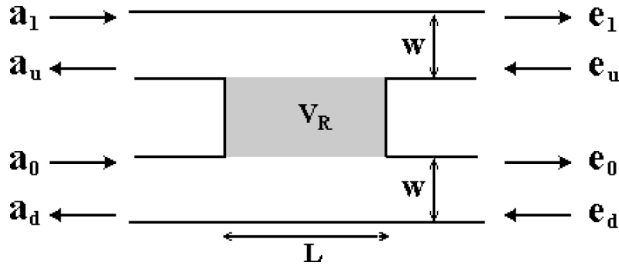


FIG. 2. The rotation gate on qubit A. The shaded region locates the potential with height V_R and length L . The width of each lead is w .

scripts u and d for the upper and lower leads, respectively, for each qubit. Probability amplitudes associated with states $|1\rangle_A$ and $|0\rangle_A$ ($|u\rangle_A$ and $|d\rangle_A$) entering qubit A on the left (right) are denoted a_1 and a_0 (e_u and e_d), respectively. Probability amplitudes associated with states $|u\rangle_A$ and $|d\rangle_A$ ($|1\rangle_A$ and $|0\rangle_A$) leaving the A qubit on the left (right) are denoted a_u and a_d (e_1 and e_0) for the upper and lower leads, respectively. Similarly, probability amplitudes associated with states $|1\rangle_B$ and $|0\rangle_B$ ($|u\rangle_B$ and $|d\rangle_B$) entering qubit B on the left (right) are denoted b_1 and b_0 (f_u and f_d), respectively. Probability amplitudes associated with states $|u\rangle_B$ and $|d\rangle_B$ ($|1\rangle_B$ and $|0\rangle_B$) leaving the B qubit on the left (right) are denoted b_u and b_d (f_1 and f_0) for the upper and lower leads, respectively.

Each qubit individually conserves probability and electrons in different qubits are distinguishable. The condition that the electron probability be conserved in qubit A is

$$(|a_1|^2 + |a_0|^2 + |e_u|^2 + |e_d|^2) = (|a_u|^2 + |a_d|^2 + |e_1|^2 + |e_0|^2), \quad (3)$$

and in qubit B it is

$$(|b_1|^2 + |b_0|^2 + |f_u|^2 + |f_d|^2) = (|b_u|^2 + |b_d|^2 + |f_1|^2 + |f_0|^2). \quad (4)$$

The probabilities in each qubit may be normalized to one without loss of generality.

Stationary states of the waveguide system in Fig. 1 can be found as follows. As a first step we note that each gate can be represented by a scattering matrix. The individual rotation gate shown in Fig. 2 has a scattering matrix \mathbf{s}_r , which connects the column matrix of incoming probability amplitudes, $\psi_{in} = (a_1, a_0, e_u, e_d)^T$, to the column matrix of outgoing probability amplitudes, $\psi_{out} = (a_u, a_d, e_1, e_0)^T$, where T denotes transpose of the row matrix. Thus, $\psi_{out} = \mathbf{s}_r \cdot \psi_{in}$ where

$$\mathbf{s}_r = \begin{pmatrix} r_{u,1} & r_{u,0} & t_{u,u} & t_{u,d} \\ r_{d,1} & r_{d,0} & t_{d,u} & t_{d,d} \\ t_{1,1} & t_{1,0} & r_{1,u} & r_{1,d} \\ t_{0,1} & t_{0,0} & r_{0,u} & r_{0,d} \end{pmatrix}. \quad (5)$$

We can also use a transfer matrix τ_r to represent the rotation gate dynamics. The transfer matrix couples the column matrix of probability amplitudes on the left, $\phi_{lft} = (a_1, a_0, a_u, a_d)^T$, to the column matrix of probability ampli-

tudes, $\phi_{rt} = (e_1, e_0, e_u, e_d)^T$, on the right. Thus, $\phi_{rt} = \tau_r \phi_{lft}$, where

$$\tau_r = \begin{pmatrix} g_{1,1} & g_{1,0} & g_{1,u} & g_{1,d} \\ g_{0,1} & g_{0,0} & g_{0,u} & g_{0,d} \\ g_{u,1} & g_{u,0} & g_{u,u} & g_{u,d} \\ g_{d,1} & g_{d,0} & g_{d,u} & g_{d,d} \end{pmatrix}. \quad (6)$$

The matrix elements in τ_r are simply related to those of the S matrix. If we write the S matrix as a 2×2 matrix of 2×2 matrices $\mathbf{s}_{1,1}$, $\mathbf{s}_{1,2}$, $\mathbf{s}_{2,1}$, and $\mathbf{s}_{2,2}$, and do the same for the transfer matrix so that

$$\mathbf{s}_r = \begin{pmatrix} \mathbf{s}_{1,1} & \mathbf{s}_{1,2} \\ \mathbf{s}_{2,1} & \mathbf{s}_{2,2} \end{pmatrix} \quad \text{and} \quad \tau_r = \begin{pmatrix} \tau_{1,1} & \tau_{1,2} \\ \tau_{2,1} & \tau_{2,2} \end{pmatrix}, \quad (7)$$

then we find

$$\begin{aligned} \tau_{11} &= \mathbf{s}_{1,1} - \mathbf{s}_{1,2} \cdot \mathbf{s}_{2,2}^{-1} \cdot \mathbf{s}_{2,1}, & \tau_{12} &= \mathbf{s}_{1,2} \cdot \mathbf{s}_{2,2}^{-1}, \\ \tau_{21} &= -\mathbf{s}_{2,2}^{-1} \cdot \mathbf{s}_{2,1}, & \tau_{22} &= \mathbf{s}_{2,2}^{-1}. \end{aligned} \quad (8)$$

These probability amplitudes can now be used to construct a transfer matrix for the entire quantum network.

When we consider the quantum network as a whole, we must take into account that it will be an entangled system. We will investigate the conditions under which it can generate measurable outgoing Bell-like states on the right given that a pair of electrons is injected into the network (one in each qubit) on the left. The network contains a Coulomb gate which entangles electrons in the two qubits so we must enlarge the space of states to allow for this entanglement. We will work in the ‘‘computational basis’’ furnished by the direct product of individual qubit basis states. Thus, we denote the state on the left of the network by the 16×1 column matrix Φ_{lft} , whose entries $\phi_{l,j}$ are the probability amplitudes associated with the state $|\Phi_{lft}\rangle$ on the left, where

$$\begin{aligned} |\Phi_{lft}\rangle &= \phi_{l,1}|1\rangle_A|1\rangle_B + \phi_{l,2}|1\rangle_A|0\rangle_B + \phi_{l,3}|1\rangle_A|u\rangle_B + \phi_{l,4}|1\rangle_A|d\rangle_B \\ &+ \phi_{l,5}|0\rangle_A|1\rangle_B + \phi_{l,6}|0\rangle_A|0\rangle_B + \phi_{l,7}|0\rangle_A|u\rangle_B \\ &+ \phi_{l,8}|0\rangle_A|d\rangle_B + \phi_{l,9}|u\rangle_A|1\rangle_B + \phi_{l,10}|u\rangle_A|0\rangle_B \\ &+ \phi_{l,11}|u\rangle_A|u\rangle_B + \phi_{l,12}|u\rangle_A|d\rangle_B + \phi_{l,13}|d\rangle_A|1\rangle_B \\ &+ \phi_{l,14}|d\rangle_A|0\rangle_B + \phi_{l,15}|d\rangle_A|u\rangle_B + \phi_{l,16}|d\rangle_A|d\rangle_B. \end{aligned} \quad (9)$$

In general $|\Phi_{lft}\rangle$ is an entangled state and this is reflected in the fact that the probability amplitudes $\phi_{l,j}$ are not separable into products of amplitudes pertaining to the individual qubits. The (entangled) state on the right of the network is given by the 16×1 column matrix Φ_{rt} , whose entries $\phi_{r,j}$ are the coefficients of the state $|\Phi_{rt}\rangle$ on the right expressed in the same basis as that of Eq. (9).

If we are given the state of the network on the left, $|\Phi_{lft}\rangle$, the ratio of probabilities $|b_1|^2$ and $|b_0|^2$ to find the electron in qubit B in state 1 or 0, respectively, is

$$\frac{|b_0|^2}{|b_1|^2} = \frac{\langle \Phi_{lft} | (|0\rangle_B \langle 0|) | \Phi_{lft} \rangle}{\langle \Phi_{lft} | (|1\rangle_B \langle 1|) | \Phi_{lft} \rangle}. \quad (10)$$

The relative phases of these two states are given by

$$\frac{b_0^* b_1}{|b_0||b_1|} = \frac{\langle \Phi_{lfi} | (|0\rangle_B \langle 1|) | \Phi_{lfi} \rangle}{\sqrt{\langle \Phi_{lfi} | (|0\rangle_B \langle 0|) | \Phi_{lfi} \rangle} \sqrt{\langle \Phi_{lfi} | (|1\rangle_B \langle 1|) | \Phi_{lfi} \rangle}}. \quad (11)$$

Similar expressions can be written for the other states on the left side of quqit B . The relative probabilities of states in quqit A can be found in an analogous manner.

The transfer matrix for each rotation gate in Fig. 1 can be represented by 16×16 transfer matrices for the network. The 16×16 transfer matrix for the rotation gate in the A quqit can be written as

$$\mathbf{R}_A = \tau_r^{(A)} \otimes \mathbf{1}_B = \begin{pmatrix} \mathbf{h}_{a,1} & \mathbf{h}_{a,0} & \mathbf{h}_{a,u} & \mathbf{h}_{a,d} \\ \mathbf{h}_{a,0} & \mathbf{h}_{a,0} & \mathbf{h}_{a,u} & \mathbf{h}_{a,d} \\ \mathbf{h}_{a,u} & \mathbf{h}_{a,u} & \mathbf{h}_{a,u} & \mathbf{h}_{a,d} \\ \mathbf{h}_{a,d} & \mathbf{h}_{a,d} & \mathbf{h}_{a,d} & \mathbf{h}_{a,d} \end{pmatrix}, \quad (12)$$

where

$$\mathbf{h}_{a,i,j} = \begin{pmatrix} g_{i,j} & 0 & 0 & 0 \\ 0 & g_{i,j} & 0 & 0 \\ 0 & 0 & g_{i,j} & 0 \\ 0 & 0 & 0 & g_{i,j} \end{pmatrix} \quad (13)$$

for $i=1,0,u,d$ and $j=1,0,u,d$. The 16×16 transfer matrix for the rotation gate in the B quqit can be written as

$$\mathbf{R}_B = \mathbf{1}_A \otimes \tau_r^{(B)} = \begin{pmatrix} \tau_r & \mathbf{0} & \mathbf{0} & \mathbf{0} \\ \mathbf{0} & \tau_r & \mathbf{0} & \mathbf{0} \\ \mathbf{0} & \mathbf{0} & \tau_r & \mathbf{0} \\ \mathbf{0} & \mathbf{0} & \mathbf{0} & \tau_r \end{pmatrix}, \quad (14)$$

where $\mathbf{0}$ is a 4×4 matrix whose elements are all zero.

The Coulomb gate, which entangles the electrons in the two quqits, can also be represented by a 16×16 matrix. We will assume that the Coulomb gate only acts when a pair of electrons is simultaneously in the states $|1\rangle_A$ and $|1\rangle_B$, or simultaneously in states $|u\rangle_A$ and $|u\rangle_B$, at the positions indicated by the shaded regions in Fig. 1. Then the 16×16 matrix \mathbf{C} represents that the Coulomb gate has matrix elements of the following form: $C_{\alpha,\beta}=1$ for $\alpha=\beta=2, \dots, 10$ and $\alpha=\beta=12, \dots, 16$; $C_{\alpha,\beta}=T_1$ for $\alpha=\beta=1$; $C_{\alpha,\beta}=T_u$ for $\alpha=\beta=11$; $C_{\alpha,\beta}=R_1$ for $\alpha=1$ and $\beta=11$; $C_{\alpha,\beta}=R_u$ for $\alpha=11$ and $\beta=1$; and $C_{\alpha,\beta}=0$ otherwise. Here T_1 (T_u) denotes the transmission probability amplitude for both electrons coming from the left (right) and R_1 (R_u) denotes the reflection probability amplitude for both electrons coming from the left (right).

We can now write the transfer matrix for the entire quantum network. If the electrons on the left side of the network are in the state Φ_{lfi} , then the outgoing electrons on the right will be in a state given by $\Phi_{rt} = \mathbf{T}_{QN} \cdot \Phi_{lfi}$, where

$$\mathbf{T}_{QN} = \mathbf{R}_B \cdot \mathbf{C} \cdot \mathbf{R}_A \cdot \mathbf{R}_B \quad (15)$$

is the transfer matrix for the entire quantum network.

Bell states are easy to obtain in idealized versions of this quantum network. For example, let us assume the rotation gates are Hadamard gates, whose S matrix is defined as $t_{1,1} = t_{1,0} = t_{0,1} = -t_{0,0} = 1/\sqrt{2}$, $r_{1,1} = r_{1,0} = r_{0,1} = r_{0,0} = 0$. We assume the Coulomb gate has the form $T_1 = -1$ and $T_u = R_1 = R_u = 0$. Let us inject a pair of electrons into the network on the left so one electron enters in the state $|1\rangle_A$ and the other electron enters in the state $|1\rangle_B$. Then $\phi_{l,1} = 1$ and $\phi_{l,j} = 0$ for $j = 2, \dots, 16$. The outgoing entangled states on the right have the probability amplitudes $\phi_{r,2} = -1/\sqrt{2}$, $\phi_{r,5} = +1/\sqrt{2}$, and $\phi_{r,j} = 0$ for $j = 1, 3, 4, 6, \dots, 16$. Thus, the incident state on the left is $|\Phi_{lfi}\rangle = |1\rangle_A |1\rangle_B$ and the transmitted state on the right is $|\Phi_{rt}\rangle = (1/\sqrt{2})(|0\rangle_A |1\rangle_B - |1\rangle_A |0\rangle_B)$, a Bell singlet state. This choice of values of transmission and reflection of the rotation gates as well as the behavior of the Coulomb gate corresponds to the idealized network in Ref. [6]. A realistic implementation of the network will include reflections from the rotation gates which impact the probability of obtaining Bell states at the output end.

The S matrices which represent the rotation gates and the Coulomb gate in the solid-state wave guide must now be determined. We must determine the actual flow of electron probability by solving the Schrödinger equation for the electron probability amplitudes in the physical devices which represent those gates. As we will see, it is only possible to obtain measurable Bell-like states under very special conditions. In the sections below, we obtain transfer matrices for both the rotation and the Coulomb gates, and we then describe the resulting Bell-like states.

III. ROTATION GATES

Rotation gates couple the pair of leads that form a quqit. Each gate is constructed by taking a pair of straight leads, which are assumed to be separated by an infinitely high potential barrier of width d , and replacing a segment of that infinite barrier by a segment of barrier of length L , width d , and potential height V_R . We need a gate that can, for example, transform an electron which enters the gate from the left in the state $|1\rangle$ to an electron which leaves the gate traveling to the right in a coherent superposition of states $|1\rangle$ and $|0\rangle$. After passage through two gates, we want the electron to emerge in the state $|0\rangle$ so that our constructed rotation gate will have properties similar to those of an ideal $\sqrt{\text{NOT}}$ gate. As we will see below, it is possible to create such a gate in the waveguide system.

The S matrix which represents the dynamics of the rotation gate is a 4×4 matrix which couples the column matrix of probability amplitudes for the incident waves, $(a_1, a_0, e_u, e_d)^T$, (T denotes transpose) to the column matrix of probability amplitudes for the outgoing waves, $(a_u, a_d, e_1, e_0)^T$. We obtained the S matrix for the rotation gate using a finite element program [17]. We use an adaptive mesh with 91 937 nodal points to approximate the wave function in the reaction region (the segment of quqit of length L which contains the potential wall, V_R). The wave function in the leads is given by $\phi(x, y) = (c/\sqrt{\kappa}) e^{i\kappa x} \phi(y)$, where c is the probability amplitude and κ is the scaled wave

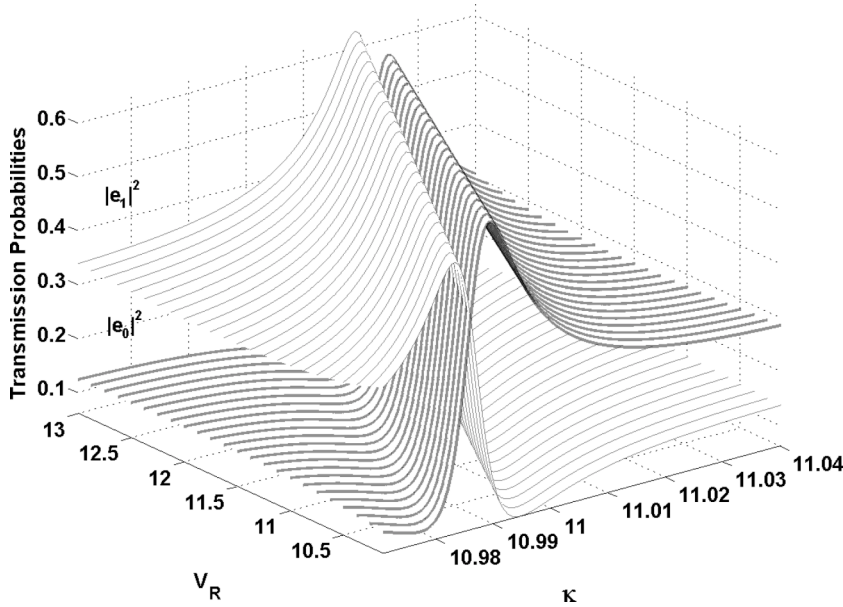


FIG. 3. The transmission probability, as a function of wave vector κ , from state $|1\rangle$ on the left to states $|1\rangle$ and $|0\rangle$ on the right for 24 different values of V_R (κ and V_R in dimensionless units). Solid thick lines represent the transmitted probability $|e_1|^2$ and solid thin lines represent transmitted probability $|e_0|^2$.

vector. We use unit current normalization. The transverse part of the wave function in each lead is $\phi(y) = \sqrt{(2/w)}\sin(\pi y/w)$, with the width of both leads equal to $w=0.4$ in dimensionless units. We require that the wave function and its first derivative be continuous at the interface between the reaction region of the gate and the leads. We have obtained transmission and reflection probability amplitudes for different values of initial wave vector with this method. Note that we only consider energies in the interval $61.7 \leq E \leq 246.8$, and we stay away from the threshold energies where new propagating channels appear, so we can neglect the evanescent modes [18,19].

Since our purpose is to obtain Bell-like states with this quantum network, the ideal rotation gate is one which completely transmits the electron wave and does not allow any reflection of the wave. We find that there are special energies at which almost complete transmission can occur. For example, let us consider the case where we send an electron into the gate from the left in the upper lead. The incident probability amplitudes are $(a_1=1, a_0=0, e_u=0, e_d=0)^T$. In Fig. 3 we show the probabilities $|e_1|^2$ and $|e_0|^2$ of the electron waves transmitted to the right as a function of barrier potential V_R . We see that the two probabilities become equal for some special values of the wave vectors. The location, in energy, of these points of equal transmission probability can be changed by changing the barrier potential V_R . Other variables that could be used to “tune” the gate are the length and width of the gate [15]. In Fig. 4 we show the probability transmitted into each of the leads for the case $V_R=11.75$.

In Fig. 5 we show the electron wave function in position space inside the reaction region of the rotation gate for the wave vector $\kappa=11.0064$, where we obtained the best behavior of the gate. The total energy for this state is $E=182.826$. For an electron incident from the left in state $|1\rangle$, we obtain transmitted probabilities $|a_u|^2=0.037$, $|a_d|^2=0.040$, $|e_1|^2=0.467$, and $|e_0|^2=0.451$. The peak in the transmission probability at this energy occurs due to a Fano resonance in the rotation gate [19]. The peak in the transmission probability

can be related to an eigenstate of a billiard with the same shape as the reaction region of the rotation gate. In Fig. 6, we show eigenstates of two billiards which closely resemble the reaction region of the rotation gate. In Fig. 6(a), we show an eigenstate of a billiard with boundary conditions such that the eigenstate is zero on the hard walls, has zero slope at the interface with the upper left lead and the two right leads, and is zero at the interface with the lower left lead. The eigenvalue of this eigenstate is $E_{15}=181.3244$. In Fig. 6(b), we show an eigenstate for a billiard with zero-slope boundary conditions at the interface with each of the leads. This state has energy $E_{15}=180.6414$. Both of the eigenstates in Fig. 6 are very close in shape and energy to the scattering state in Fig. 5, a clear indication that we are observing a Fano resonance.

We have also calculated the Wigner delay times of the scattered waves over the entire energy interval $61.7 \leq E \leq 246.8$. The Wigner delay time is defined as the average slope (as a function of energy) of the S -matrix eigenphases.

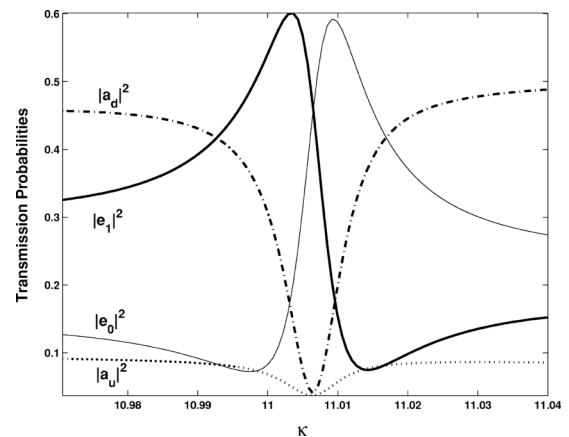


FIG. 4. The probability of transmitted and reflected waves, $|e_1|^2$, $|e_0|^2$, $|a_u|^2$, $|a_d|^2$, as a function of incident wave vector κ for $V_R=11.75$ (κ and V_R in dimensionless units). A plane wave with unit amplitude is incident from the left in state $|1\rangle$.

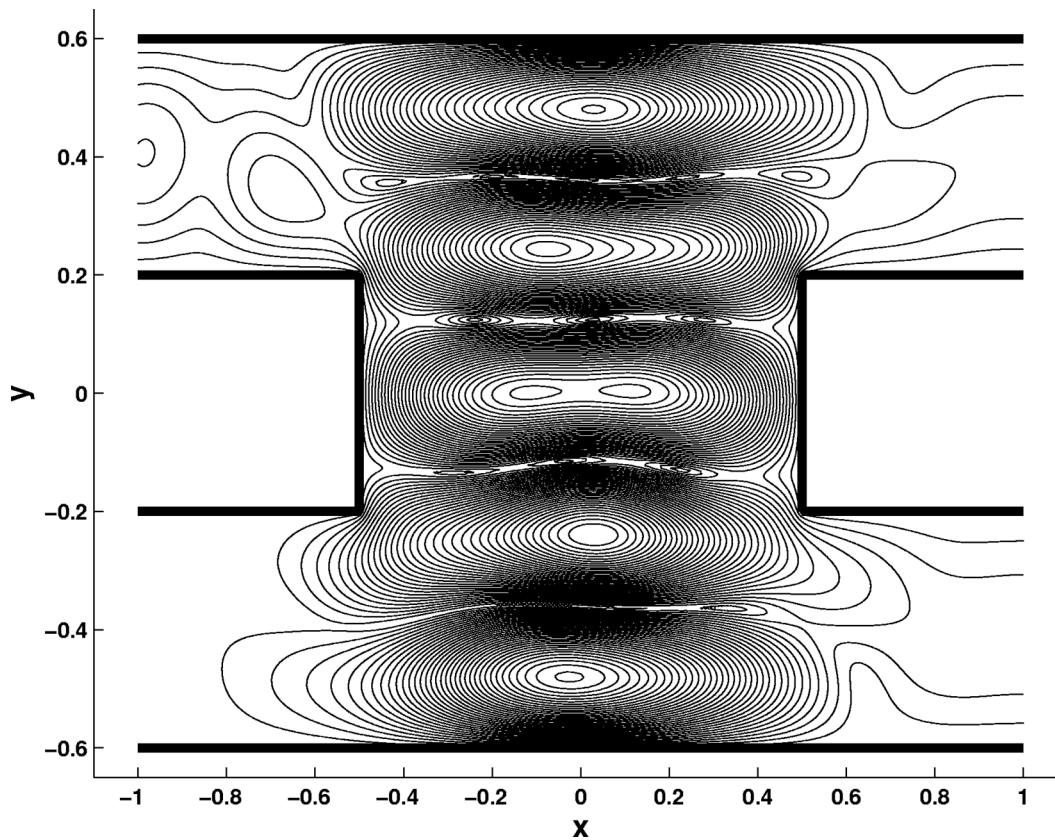


FIG. 5. Probability distribution of electron wave function in configuration space (x, y) inside the rotation gate at resonance for the case when a plane wave is incident from the left in state $|1\rangle$. Here $V_R=11.75$ and $\kappa=11.0064$ (κ , V_R , x , and y in dimensionless units).

It is plotted as a function of energy in the interval $61.7 \leq E \leq 246.8$ in Fig. 7. There are five prominent delay time peaks but the largest occurs at the energy $E=182.826$, where the rotation gate exhibits a Fano resonance. At this energy there

is almost perfect transmission, but there is also an extra long delay time associated with the transmission resonance.

The S matrix for the rotation gate, at the resonance energy $E=182.826$ and wave vector $\kappa=11.006$, is given by

$$S_{h,res} = \begin{pmatrix} -0.1902 + 0.0254i & 0.1774 - 0.1116i & -0.6398 - 0.3050i & -0.3190 + 0.5571i \\ 0.1774 - 0.1116i & -0.1912 + 0.0255i & -0.3192 + 0.5567i & -0.6397 - 0.3051i \\ -0.6398 - 0.3050i & -0.3192 + 0.5567i & -0.1951 + 0.0260i & 0.1733 - 0.1104i \\ -0.3190 + 0.5571i & -0.6397 - 0.3051i & 0.1733 - 0.1104i & -0.1947 + 0.0269i \end{pmatrix}. \quad (16)$$

This S matrix was obtained using the finite element method described in the beginning of this section. It is useful for our subsequent discussion to give an S matrix at incident wave vector $\kappa=10.902$, which is off-resonance. The S matrix at $\kappa=10.902$ is

$$S_{h,nonres} = \begin{pmatrix} -0.6629 + 0.0769i & 0.3111 + 0.0351i & -0.0439 + 0.3667i & 0.0663 - 0.5620i \\ 0.3114 + 0.0350i & 0.6629 + 0.0769i & 0.0662 - 0.5617i & -0.0439 + 0.3670i \\ -0.0439 + 0.3670i & 0.0663 - 0.5620i & 0.6629 + 0.0764i & 0.3108 + 0.0348i \\ 0.0662 - 0.5617i & -0.0439 + 0.3667i & 0.3116 + 0.0349i & 0.6629 + 0.0764i \end{pmatrix}. \quad (17)$$

These S matrices are accurate to three significant figures.

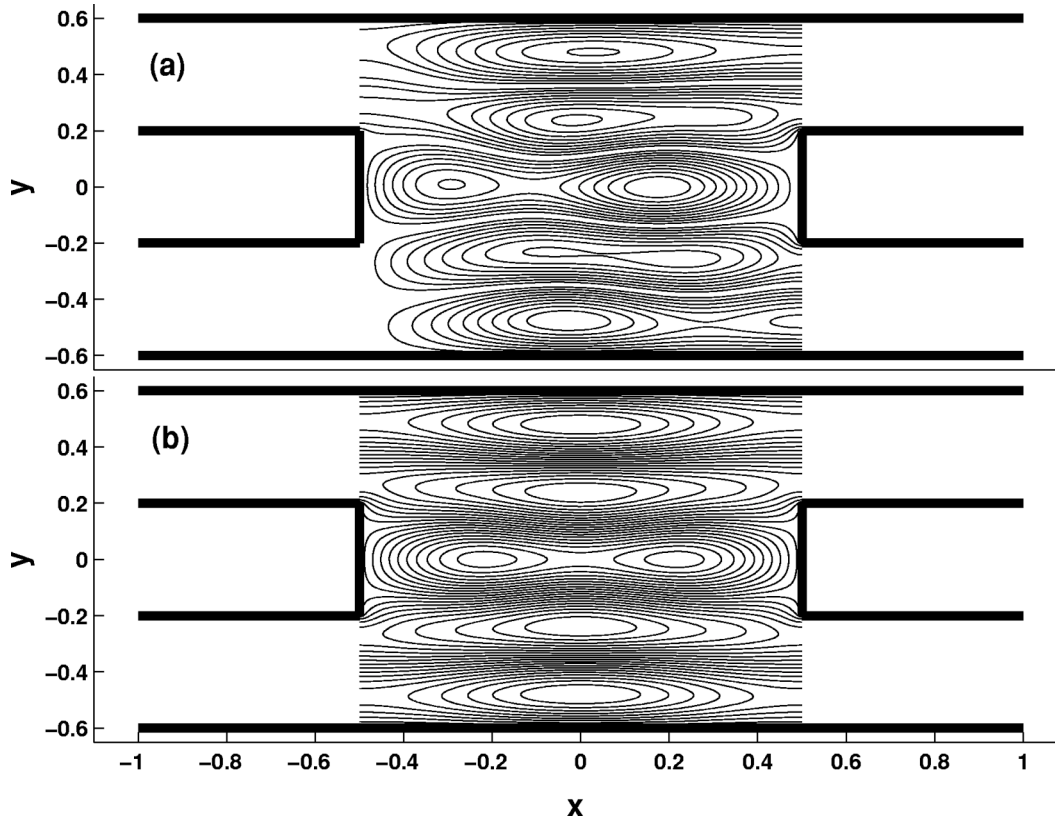


FIG. 6. The eigenfunctions of billiards whose interior regions are shaped like that of the rotation gates for the case $V_R=11.75$. (a) The 15th eigenstate with zero-slope boundary conditions at $x=-L/2$ for the upper lead and at $x=\pm L/2$ in both leads, and zero wave function at $x=-L/2$ on the lower lead. The eigenvalue of this state is $E=181.3244$. (b) The 15th eigenstate with zero-slope boundary conditions at $x=-L/2$ in both leads and at $x=\pm L/2$ in both leads. The eigenvalue of this state is $E=180.6414$ (x , y , V_R , and E in dimensionless units).

We will operate the quantum network at energy $E=182.826$ and wave vector $\kappa=11.006$ where the rotation gate has its best performance for the geometry we have chosen. However, before discussing the behavior of the quantum network, we must first discuss a possible way to entangle the two quqits which comprise the network.

IV. THE COULOMB GATE

We wish to entangle the electron states in the two quqits but not allow the electrons to pass between the quqits. Ideally we can accomplish this by using the Coulomb interaction between the electrons in the two quqits [20].

Quantum computing algorithms rely on “accurate” unitary transformations. The quantum gates must impart reasonably precise phases to the electrons for the computation to be successful. To obtain measurable Bell states for this network, the gates must minimize reflection. In this section, we suggest a simple design for a Coulomb gate which would minimize reflection and maximize phase precision.

The simplest form of Coulomb gate consists of a section of the upper leads of the two quqits of length $2\Delta x$ (in dimensionless units), where the Coulomb interaction between two electrons traveling in those leads (one in each lead) can be activated. In order for the Coulomb gate to work, we must simultaneously have electrons in states $|1\rangle_A$ and $|1\rangle_B$ (or in

$|u\rangle_A$ and $|u\rangle_B$) in that region of space. We assume that the upper leads of the two quqits are separated by a distance D . We also assume that the two electrons have the same momentum κ and enter the gate together. If the distance between the leads, D , is large compared to the width of the leads, w , we can approximate the dynamics by that of two electrons moving in parallel one-dimensional quantum wires. If the two electrons enter the interaction region at the same time with the same initial momentum, the repulsive Coulomb force between the electrons will be perpendicular to their motion. The potential generated in the each of the leads by the electron in the other lead is approximately a constant V_C (in dimensionless units), within the interaction window $-\Delta x$ to $+\Delta x$ and zero elsewhere. The strength of the potential is proportional to the inverse of the distance between the leads.

Restricting our attention to just one of the electrons traveling through the Coulomb gate, we model the potential induced by the other electron as a simple step potential, and treat the situation as a single electron in one dimension scattering off of the step potential. The step potential is given by

$$V = \begin{cases} V_C & \text{if } -\Delta x \leq x \leq +\Delta x, \\ 0 & \text{elsewhere.} \end{cases} \quad (18)$$

If the initial energy of the electron satisfies the condition $E > V_C + (\pi/0.4)^2$, then the transmission probability amplitude is given by

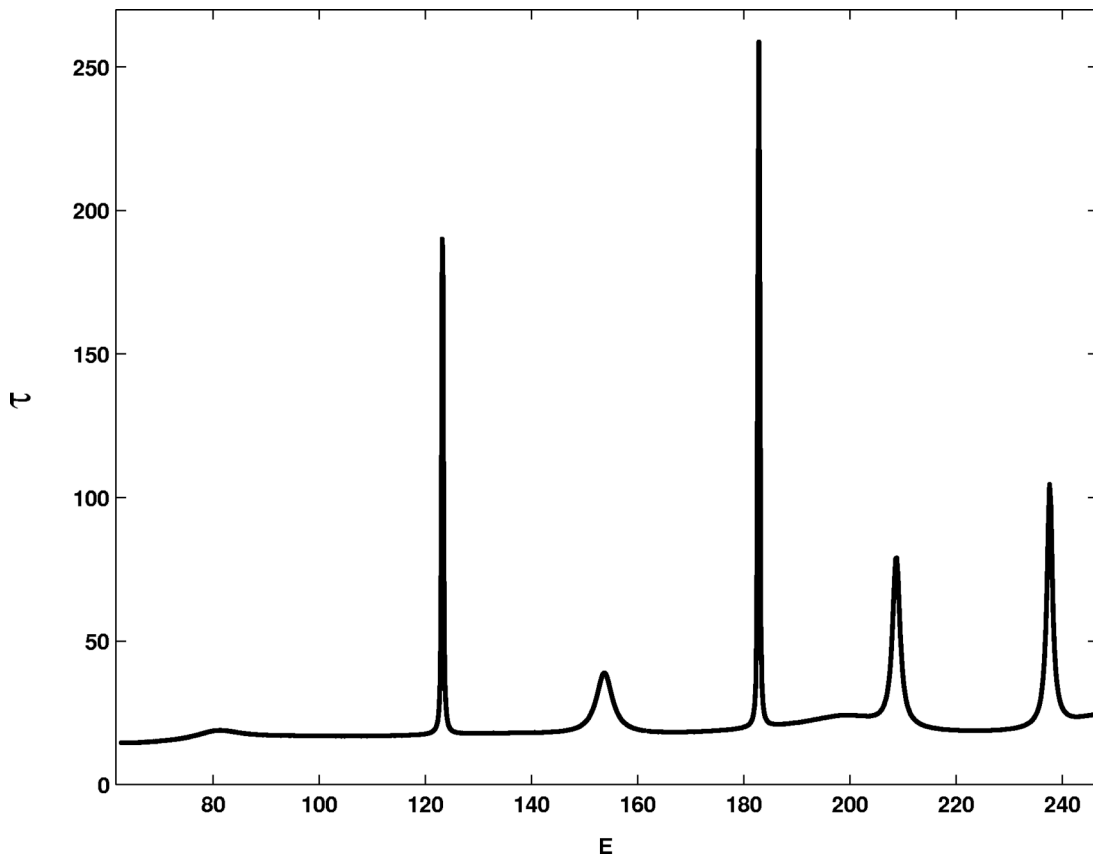


FIG. 7. The Wigner delay time τ as a function of energy for the energy interval $61.7 \leq E \leq 246.7$ with $V_R=11.75$ (τ , E , and V_R in dimensionless units).

$$T = \frac{-4e^{-2i(\kappa-l)\Delta x}\kappa l}{e^{4il\Delta x}(\kappa-l)^2 - (\kappa+l)^2}, \quad (19)$$

where κ is the wave vector of the electron in the lead and l is the wave vector in the potential region,

$$l^2 = E - V_C - \left(\frac{\pi}{0.4}\right)^2. \quad (20)$$

The transmission probability $|T|^2$ is, in general, less than 1. However, there are transmission resonances when $l\Delta x = \nu\pi/2$, where $\nu=0, 1, 2, \dots, \infty$. When this condition is satisfied there is total transmission at energies

$$E = \left(\frac{\nu\pi}{2\Delta x}\right)^2 + V_C + \left(\frac{\pi}{0.4}\right)^2. \quad (21)$$

Not only do we seek total transmission, but we also wish to impart a specific phase to the electron as it travels through the Coulomb gate. At resonances, the transmission amplitude reduces to

$$T = (-1)^\nu e^{-2i\kappa\Delta x} = (-1)^\nu e^{-i\phi}, \quad (22)$$

where $\phi=2\kappa\Delta x$ is phase change of the electron wave when it passes through the step potential.

Let us now assume that the electrons have Fermi energy $E=182.826$, which is the energy at which we wish to operate the rotation gate. Thus, in the subsequent analysis of the

Coulomb gate, we fix the energy to be $E=182.826$ and find values for the height of the potential step V_C and the length of the interaction $2\Delta x$ that will provide total transmission with a specific value of the phase angle $\phi=2\kappa\Delta x$. From above we find

$$\Delta x = \frac{-\phi}{2\sqrt{E - \left(\frac{\pi}{0.4}\right)^2}}$$

$$\text{with } V_C = \left[E - \left(\frac{\pi}{0.4}\right)^2 \right] \left[1 - \left(\frac{\nu\pi}{\phi}\right)^2 \right] \quad (23)$$

for specific values of E and ϕ . The phase angle should be less than zero, $\phi < 0$, so that Δx is positive. Using the fact that $T(\phi) = T(\phi - 2\pi)$, we can adjust the phase angle ϕ and the mode number ν to obtain the desired values of V_C . Once the value of V_C is set, we can find the separation distance D required between the quqits to produce such a potential, given that the Coulomb potential can be written as

$$V_C = \frac{1}{4\pi\epsilon_0} \frac{e^2}{D E_o}, \quad (24)$$

where we have assumed the limit of a perfect dielectric between the leads.

As an example of a possible Coulomb gate, we select $\nu = 3$ and a phase angle $\phi = -7\pi/2$. Then the length of the gate is $2\Delta x = 0.999$ in dimensionless units and the potential height generated by the two electrons is $V_C = 32.139$, which corresponds to a distance between the leads of $D = 1.572$ in dimensionless units. This gives a transmission amplitude of $t = i$ for each electron and no reflection. Thus, for the Coulomb gate in Sec. II, we take $T_l = -1$, $T_u = -1$, $R_l = 0$, and $R_u = 0$.

V. STATIONARY STATES OF THE QUANTUM NETWORK

As we shall see, actually controlling the input and output of the quantum network is not straightforward. For simplicity let us take the simplest possible state on the left, $\Phi_{lft} = (1, 0, 0, 0, 0, 0, 0, 0, 0, 0, 0, 0, 0, 0, 0, 0)^T$. This state is somewhat unphysical because it assumes that there is no reflection back to the left. We can construct the transfer matrix at the resonance energy $E = 182.826$, using the S matrix in Eq. (16) and the Coulomb coupler described above. We then find that the probability amplitudes on the right are given by

$$\begin{aligned} \Phi_{rt} = & (0.016 + 0.800i, 0.0589 + 0.0330i, 0.148 - 0.0536i, \\ & -0.167 - 0.010i, -0.115 + 0.011i, 0.168 + 0.691i, \\ & \times 0.052 + 0.017i, -0.154 - 0.078i, -0.024 \\ & + 0.005i, 0.112 + 0.146i, -0.025 + 0.022i, -0.061 \\ & -0.036i, 0.037 - 0.021i, -0.158 - 0.207i, \\ & -0.020 + 0.002i, 0.063 + 0.004i)^T. \end{aligned} \quad (25)$$

Thus, on the right we have a state

$$\begin{aligned} |\Phi_{rt}\rangle = & (0.016 + 0.800i)|1\rangle_A|1\rangle_B + (0.168 + 0.691i)|0\rangle_A|0\rangle_B \\ & + \dots, \end{aligned} \quad (26)$$

which is predominantly an entangled Bell-like triplet state. However, there is a small amount electron flow entering from the right which we would like to avoid. Below we give an alternate means to determine the allowed stationary states in the network which allow a more systematic search of allowed states of the network.

A possible analog of this network in quantum information theory is the one which uses a $\sqrt{\text{NOT}}$ gate with transmission probability amplitudes $t_{1,1} = t_{0,0} = t_{u,u} = t_{d,d} = -(1+i)/2$ and $t_{1,0} = t_{0,1} = t_{u,d} = t_{d,u} = -(1-i)/2$ and reflection probability amplitudes $r_{i,j} = 0$ with $i = 1, 0$ and $j = 1, 0$ and $r_{i,j} = 0$ with $i = u, d$ and $j = u, d$. This ideal quantum network acting on the state $\Phi_{lft} = (1, 0, 0, 0, 0, 0, 0, 0, 0, 0, 0, 0, 0, 0, 0, 0)^T$ gives exactly the state

$$|\Phi_{rt}\rangle = (-0.5 + 0.5i)|1\rangle_A|1\rangle_B + (-0.5 + 0.5i)|0\rangle_A|0\rangle_B, \quad (27)$$

which is a Bell state.

The transfer matrix \mathbf{T}_{QN} in Eq. (15) is a useful tool for computing the output of the network on the right for given input on the left. However, as a tool to explore the global properties of the network, the transfer matrix \mathbf{T}_{QN} is an unwieldy object primarily because it does not preserve the norm of the states it acts on (it is not unitary). It is therefore

desirable to find a unitary matrix that characterizes the behavior of the network. An obvious choice for such a unitary matrix would be an S matrix which connects the incoming states of the network to outgoing states of the network. However, the basis states that would be necessary for construction of a network S matrix are not available to us. The basis states we would need would include states such as $|1\rangle_A^L \otimes |u\rangle_B^R$ where L and R stand for left and right ends of the network, respectively, but we have no information about these states. The transfer matrix \mathbf{T}_{QN} connects states of the form $|^L \otimes |^L$ to states of the form $|^R \otimes |^R$. Unless the coefficients that appear in the expansions of $|\Phi_{lft}\rangle$ and $|\Phi_{rt}\rangle$ in the computational basis are separable into products of two independent amplitudes we cannot extract the amplitudes of states of the form $|^L \otimes |^R$ by knowing just the transfer matrix of the network. Entanglement indeed means that the coefficients $\phi_{l,i}$ and $\phi_{r,i}$ of $|^L \otimes |^L$ and $|^R \otimes |^R$, respectively, are not separable into products of single-qubit state amplitudes. The presence of entangling operations in the network prevents us from identifying an S matrix that characterizes the network starting from the transfer matrix. However, as we shall show below, it is possible to obtain a unitary matrix for the entire network which explicitly conserves probability.

A. Construction of a unitary matrix

The unitary matrix \mathbf{U}_{QN} which characterizes the dynamics of the quantum network has a very different structure from that of the transfer matrix \mathbf{T}_{QN} . We can obtain the unitary matrix from the transfer matrix via a series of transformations. These transformations involve a considerable rearrangement of elements of the network states. The rearranged network states are given by $|\Xi_1\rangle$ and $|\Xi_2\rangle$, where

$$\begin{aligned} |\Xi_1\rangle = & \phi_{l,1}|1\rangle_A|1\rangle_B + \phi_{l,2}|1\rangle_A|0\rangle_B + \phi_{r,3}|1\rangle_A|u\rangle_B + \phi_{r,4}|1\rangle_A|d\rangle_B \\ & + \phi_{l,5}|0\rangle_A|1\rangle_B + \phi_{l,6}|0\rangle_A|0\rangle_B + \phi_{r,7}|0\rangle_A|u\rangle_B \\ & + \phi_{r,8}|0\rangle_A|d\rangle_B + \phi_{r,9}|u\rangle_A|1\rangle_B + \phi_{r,10}|u\rangle_A|0\rangle_B \\ & + \phi_{l,11}|u\rangle_A|u\rangle_B + \phi_{l,12}|u\rangle_A|d\rangle_B + \phi_{r,13}|d\rangle_A|1\rangle_B \\ & + \phi_{r,14}|d\rangle_A|0\rangle_B + \phi_{l,15}|d\rangle_A|u\rangle_B + \phi_{l,16}|d\rangle_A|d\rangle_B \end{aligned} \quad (28)$$

and

$$\begin{aligned} |\Xi_2\rangle = & \phi_{r,1}|1\rangle_A|1\rangle_B + \phi_{r,2}|1\rangle_A|0\rangle_B + \phi_{l,3}|1\rangle_A|u\rangle_B + \phi_{l,4}|1\rangle_A|d\rangle_B \\ & + \phi_{r,5}|0\rangle_A|1\rangle_B + \phi_{r,6}|0\rangle_A|0\rangle_B + \phi_{l,7}|0\rangle_A|u\rangle_B \\ & + \phi_{l,8}|0\rangle_A|d\rangle_B + \phi_{l,9}|u\rangle_A|1\rangle_B + \phi_{l,10}|u\rangle_A|0\rangle_B \\ & + \phi_{r,11}|u\rangle_A|u\rangle_B + \phi_{r,12}|u\rangle_A|d\rangle_B + \phi_{l,13}|d\rangle_A|1\rangle_B \\ & + \phi_{l,14}|d\rangle_A|0\rangle_B + \phi_{r,15}|d\rangle_A|u\rangle_B + \phi_{r,16}|d\rangle_A|d\rangle_B. \end{aligned} \quad (29)$$

An explanation of how we choose these states is given in the Appendix. The unitary matrix \mathbf{U}_{QN} which connects these states satisfies the condition $\Xi_2 = \mathbf{U}_{QN}\Xi_1$.

The unitary matrix \mathbf{U}_{QN} can be obtained from the transfer matrix \mathbf{T}_{QN} as follows. First write the transfer matrix \mathbf{T}_{QN} as a 2×2 matrix containing the four 8×8 matrices F_{11} , F_{12} , F_{21} , and F_{22} as its matrix elements so that

$$\mathbf{T}_{QN} = \begin{pmatrix} F_{11} & F_{12} \\ F_{21} & F_{22} \end{pmatrix}. \quad (30)$$

Then introduce a new matrix,

$$\mathbf{G} = \begin{pmatrix} G_{11} & G_{12} \\ G_{21} & G_{22} \end{pmatrix}, \quad (31)$$

whose matrix elements are defined as

$$G_{11} = F_{11} - F_{12}F_{22}^{-1}F_{21}, \quad G_{12} = F_{12}F_{22}^{-1},$$

$$G_{21} = -F_{22}^{-1}F_{21}, \quad G_{22} = F_{22}^{-1}.$$

Next introduce a matrix \mathbf{K} which can be written as a 2×2 matrix of 8×8 matrices K_{11} , K_{12} , K_{21} , and K_{22} so that

$$\mathbf{K} = \begin{pmatrix} K_{11} & K_{12} \\ K_{21} & K_{22} \end{pmatrix}. \quad (32)$$

Each of the matrices K_{11} , K_{12} , K_{21} , and K_{22} can be written as a 4×4 matrix whose matrix elements are 2×2 matrices $g_{m,n}$ as follows:

$$\begin{aligned} K_{11} &= \begin{pmatrix} g_{1,1} & g_{1,3} & g_{1,5} & g_{1,7} \\ g_{3,1} & g_{3,3} & g_{3,5} & g_{3,7} \\ g_{5,1} & g_{5,3} & g_{5,5} & g_{5,7} \\ g_{7,1} & g_{7,3} & g_{7,5} & g_{7,7} \end{pmatrix}, \\ K_{12} &= \begin{pmatrix} g_{1,2} & g_{1,4} & g_{1,6} & g_{1,8} \\ g_{3,2} & g_{3,4} & g_{3,6} & g_{3,8} \\ g_{5,2} & g_{5,4} & g_{5,6} & g_{5,8} \\ g_{7,2} & g_{7,4} & g_{7,6} & g_{7,8} \end{pmatrix}, \\ K_{21} &= \begin{pmatrix} g_{2,1} & g_{2,3} & g_{2,5} & g_{2,7} \\ g_{4,1} & g_{4,3} & g_{4,5} & g_{4,7} \\ g_{6,1} & g_{6,3} & g_{6,5} & g_{6,7} \\ g_{8,1} & g_{8,3} & g_{8,5} & g_{8,7} \end{pmatrix}, \\ K_{22} &= \begin{pmatrix} g_{2,2} & g_{2,4} & g_{2,6} & g_{2,8} \\ g_{4,2} & g_{4,4} & g_{4,6} & g_{4,8} \\ g_{6,2} & g_{6,4} & g_{6,6} & g_{6,8} \\ g_{8,2} & g_{8,4} & g_{8,6} & g_{8,8} \end{pmatrix}. \end{aligned} \quad (33)$$

The 2×2 matrices $g_{m,n}$ are defined as

$$g_{m,n} = \begin{pmatrix} \mathbf{G}_{2m-1,2n-1} & \mathbf{G}_{2m-1,2n} \\ \mathbf{G}_{2m,2n-1} & \mathbf{G}_{2m,2n} \end{pmatrix}, \quad (34)$$

where $m, n = 1, \dots, 8$.

In the next step we introduce matrix \mathbf{M} which can be written as a 2×2 matrix of 8×8 matrices M_{11} , M_{12} , M_{21} , and M_{22} such that

$$\mathbf{M} = \begin{pmatrix} M_{11} & M_{12} \\ M_{21} & M_{22} \end{pmatrix}, \quad (35)$$

where

$$M_{11} = K_{11} - K_{12}K_{22}^{-1}K_{21}, \quad M_{12} = K_{12}K_{22}^{-1},$$

$$M_{21} = -K_{22}^{-1}K_{21}, \quad M_{22} = K_{22}^{-1}.$$

It is useful to introduce 2×2 submatrices of the matrix \mathbf{M} defined as

$$\mu_{m,n} = \begin{pmatrix} \mathbf{M}_{2m-1,2n-1} & \mathbf{M}_{2m-1,2n} \\ \mathbf{M}_{2m,2n-1} & \mathbf{M}_{2m,2n} \end{pmatrix}. \quad (36)$$

Then in terms of these 2×2 submatrices, the unitary matrix \mathbf{U}_{QN} for the quantum network finally can be written as

$$\mathbf{U}_{QN} = \begin{pmatrix} U_{11} & U_{12} \\ U_{21} & U_{22} \end{pmatrix}, \quad (37)$$

where

$$\begin{aligned} U_{11} &= \begin{pmatrix} \mu_{1,1} & \mu_{1,5} & \mu_{1,2} & \mu_{1,6} \\ \mu_{5,1} & \mu_{5,5} & \mu_{5,2} & \mu_{5,6} \\ \mu_{2,1} & \mu_{2,5} & \mu_{2,2} & \mu_{2,6} \\ \mu_{6,1} & \mu_{6,5} & \mu_{6,2} & \mu_{6,6} \end{pmatrix}, \\ U_{12} &= \begin{pmatrix} \mu_{1,3} & \mu_{1,7} & \mu_{1,4} & \mu_{1,8} \\ \mu_{5,3} & \mu_{5,7} & \mu_{5,4} & \mu_{5,8} \\ \mu_{2,3} & \mu_{2,7} & \mu_{2,4} & \mu_{2,8} \\ \mu_{6,3} & \mu_{6,7} & \mu_{6,4} & \mu_{6,8} \end{pmatrix}, \\ U_{21} &= \begin{pmatrix} \mu_{3,1} & \mu_{3,5} & \mu_{3,2} & \mu_{3,6} \\ \mu_{7,1} & \mu_{7,5} & \mu_{7,2} & \mu_{7,6} \\ \mu_{4,1} & \mu_{4,5} & \mu_{4,2} & \mu_{4,6} \\ \mu_{8,1} & \mu_{8,5} & \mu_{8,2} & \mu_{8,6} \end{pmatrix}, \\ U_{22} &= \begin{pmatrix} \mu_{3,3} & \mu_{3,7} & \mu_{3,4} & \mu_{3,8} \\ \mu_{7,3} & \mu_{7,7} & \mu_{7,4} & \mu_{7,8} \\ \mu_{4,3} & \mu_{4,7} & \mu_{4,4} & \mu_{4,8} \\ \mu_{8,3} & \mu_{8,7} & \mu_{8,4} & \mu_{8,8} \end{pmatrix}. \end{aligned} \quad (38)$$

As we show below, the eigenstates of the unitary matrix give us a new way to obtain the allowed states of the network.

B. Eigenvalues and eigenstates of \mathbf{U}_{QN}

Because the eigenstates of the unitary matrix \mathbf{U}_{QN} form a complete orthonormal set, we can use them to obtain allowed states of the network whose physical properties are as close as possible to those we seek. We can expand the states Ξ_1 and Ξ_2 in terms of the complete set of eigenstates of \mathbf{U}_{QN} . By properly selecting the coefficients in the eigenstate expansions, we can obtain various allowed states of the quantum network. As an example we have found an alternative to the state $\Phi_{lft} = (1, 0, 0, 0, 0, 0, 0, 0, 0, 0, 0, 0, 0, 0, 0, 0)^T$ (which does not allow reflection to the left) and the resulting state Φ_{rt} presented in Eq. (25). If we use an expansion in terms of eigenstates of \mathbf{U}_{QN} as described above we can obtain the following states:

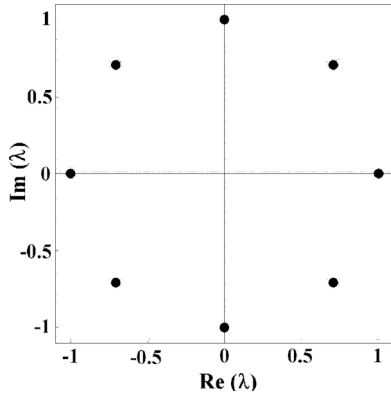


FIG. 8. Eigenvalues λ of the unitary matrix \mathbf{U}_{QN} for $\sqrt{\text{NOT}}$ gates with S -matrix elements $t_{i,i} = -(1+i)/2$, $t_{i,j} = -(1-i)/2$ ($i \neq j$), and $r_{i,j} = 0$.

$$\begin{aligned} \Phi_{ff} = & (1.0, 0, 0.096 - 0.001i, -0.025 - 0.087i, 0, 0, \\ & -0.167 + 0.032i, 0.108 - 0.042i, -0.190 \\ & + 0.025i, 0, -0.008 + 0.022i, 0.011 \\ & - 0.002i, 0.177 - 0.112i, 0, 0.014 + 0.0003i, \\ & -0.025 - 0.008i)^T, \end{aligned} \quad (39)$$

$$\begin{aligned} \Phi_{rr} = & (0.068 + 0.676i, -0.036 + 0.036i, 0, 0, -0.095 \\ & + 0.022i, 0.089 + 0.605i, 0, 0, 0, 0, 0, 0, 0, 0)^T. \end{aligned} \quad (40)$$

The states in Eqs. (39) and (40) do not allow electrons to enter from the right. They do allow electrons to leave on the left and right. There is a small amount of electron probability incident in the $|0\rangle$ state of the A quqit but none in $|0\rangle$ state of the B quqit. This more physical state also gives rise to measurable Bell states leaving the network on the right.

It is of interest to study the behavior of the eigenvalues of the unitary matrix \mathbf{U}_{QN} . The manner in which they are dis-

tributed on the unit circle can give some information about the nature of the network dynamics. A high degree of degeneracy in the eigenvalues can be an indicator that underlying symmetries are playing a role in the dynamics. As an example, let us consider a quantum network whose rotation gate dynamics is given by the $\sqrt{\text{NOT}}$ gate. For this system, there is no coupling between right and left flow on the network and we expect a high degree of degeneracy in the eigenvalues of \mathbf{U}_{QN} . This can be seen in Fig. 8 where we plot the eigenvalues of \mathbf{U}_{QN} on the unit circle. There are eight distinct eigenvalues, each of which is two-fold degenerate.

More realistic choices of S matrices for the rotation gates are the ones given in Eqs. (16) and (17) for resonant and nonresonant flow through the gates. These were computed by solving the Schrödinger equation. These S matrices do allow reflection. We construct \mathbf{U}_{QN} as described earlier out of the transfer matrices obtained for the network with these choices of S matrix for the rotation gates. For both cases, the Coulomb gate can be adjusted to give a phase shift of i to both electrons with no reflection. The eigenvalues of \mathbf{U}_{QN} for the resonant and nonresonant cases are shown in Fig. 9. For these cases, which now allow reflection, all the degeneracy has been lifted.

In the following section, we choose a simplified one parameter family of real S matrices for the rotation gates and systematically explore the effect of introducing reflections at the rotation gates on the eigenvalues of \mathbf{U}_{QN} .

VI. BROKEN SYMMETRY ON THE QUANTUM NETWORK

We can systematically study the effect of reflection on the eigenvalue spectrum of \mathbf{U}_{QN} for a case where we can parametrize the degree of reflection on the network by a single real parameter b . We introduce a real S matrix for the individual rotation gates with the form

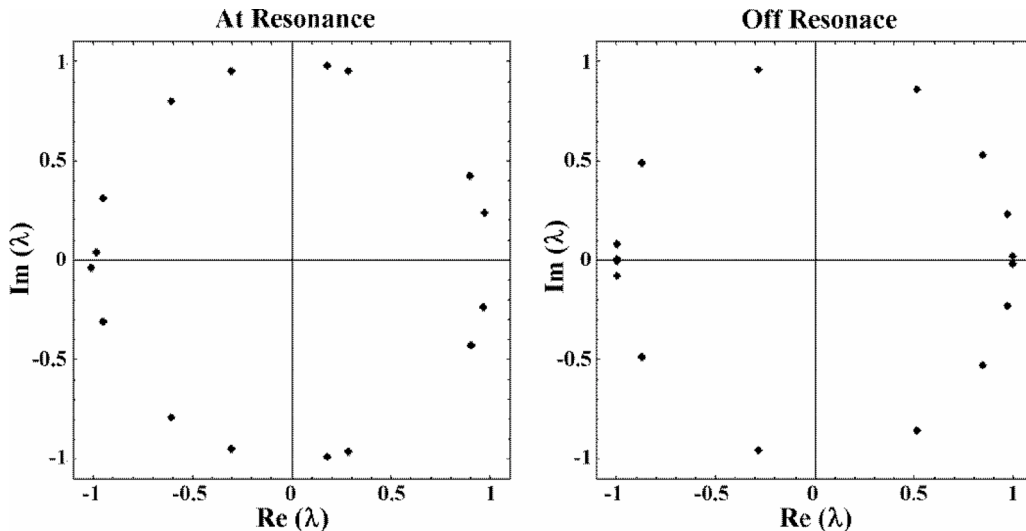


FIG. 9. Eigenvalues λ of \mathbf{U}_{QN} for the resonant rotation gate $s_{r,res}(\kappa=11.006)$ and the nonresonant rotation gate $s_{r,nonres}(\kappa=10.902)$.

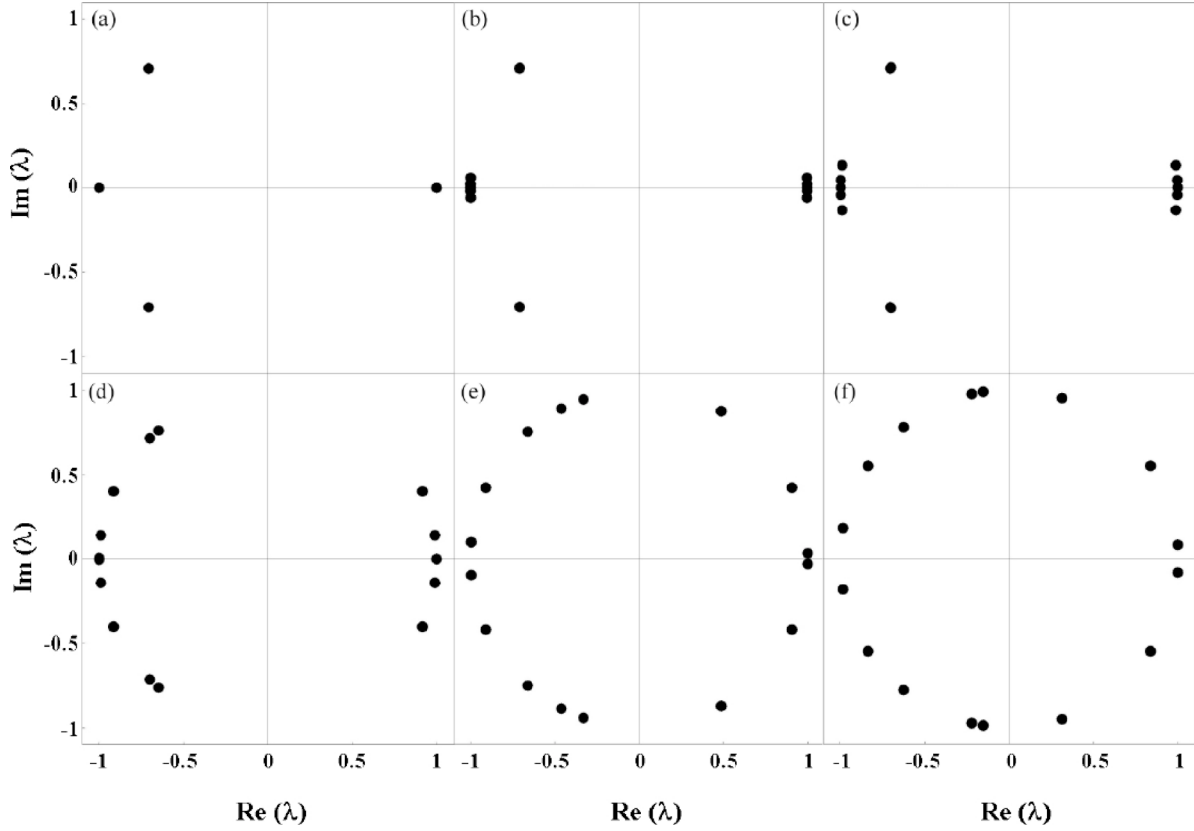


FIG. 10. Eigenvalues λ of \mathbf{U}_{QN} for rotation gates with S matrix $s_{r,b}$ [see Eq. (41)]. (a) $b=0$, (b) $b=\frac{1}{5000}$, (c) $b=\frac{1}{1000}$, (d) $b=\frac{1}{100}$, (e) $b=\frac{1}{50}$, and (f) $b=\frac{1}{5}$.

$$\mathbf{s}_{h,b} = \begin{pmatrix} \sqrt{2}\sqrt{b-b^2} & b & (1-b)\sqrt{2} & (1-b)\sqrt{2} \\ -b & \sqrt{2}\sqrt{b-b^2} & (1-b)\sqrt{2} & -(1-b)\sqrt{2} \\ (1-b)\sqrt{2} & (1-b)\sqrt{2} & -\sqrt{2}\sqrt{b-b^2} & -b \\ (1-b)\sqrt{2} & -(1-b)\sqrt{2} & b & -\sqrt{2}\sqrt{b-b^2} \end{pmatrix}. \quad (41)$$

For the case $b=0$, this S matrix reduces to a Hadamard gate. The change in the eigenvalue spectrum as b increases is shown in Fig. 10. For the case $b=0$, which has no reflection, the eigenvalues of the matrix \mathbf{U}_{QN} are highly degenerate. They are given by $\lambda=-1$ (six-fold degenerate), $\lambda=+1$ (six-fold degenerate), $\lambda=-(1+i)/\sqrt{2}$ (two-fold degenerate), and $\lambda=(-1+i)/\sqrt{2}$ (two-fold degenerate). However, as we increase the value of b from zero the degeneracy of the eigenvalues is broken. Above a certain value of b we start to see strong level repulsion, an indicator that the directional symmetries of the network are clearly broken.

We can also compute a type of fidelity to the pure Bell state for this quantum network. We define the fidelity F of the quantum network as

$$F = |\langle \Phi_{rt}^{(0)} | \Phi_{rt}^{(b)} \rangle|^2, \quad (42)$$

where $|\Phi_{rt}^{(0)}\rangle$ is the output of the network for $b=0$. A plot of the fidelity as a function of b is given in Fig. 11. We see that

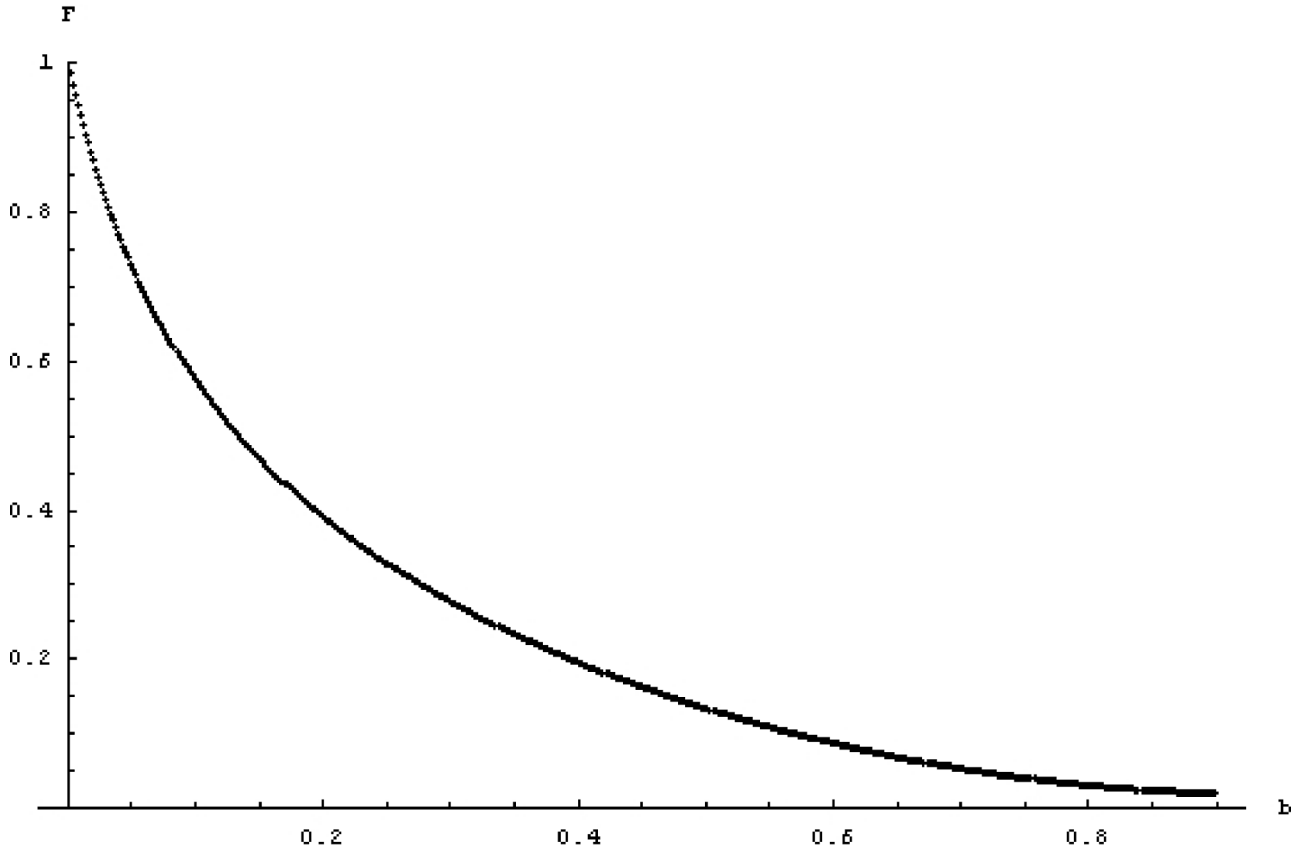
as we increase the amount of reflection, as measured by the parameter b , the fidelity decreases exponentially with b .

VII. CONCLUSION

We have studied the dynamics of an entangled quantum network consisting of two qubits constructed from hard wall ballistic electron waveguides. We have studied the stationary states of the waveguide network, rather than the behavior of wave packets [6,7], because the stationary states are more closely linked to the measurable conduction properties of such a network. The properties of our gates are determined from the actual flow properties of electron matter waves in waveguides constructed from GaAs/Al_xGa_{1-x}As heterostructures. The sizes of gates and the electron energies are realistic for those systems. Our goal was to determine if it is possible to generate Bell-like states with such a network. We have found that, when the network is run at resonance where reflection is minimized, Bell-like states can be generated.

ACKNOWLEDGMENTS

G.B.A., L.E.R., and M.G.S. wish to thank the Robert A. Welch Foundation (Grant No. F-1051) and the Engineering Research Program of the Office of Basic Energy Sciences at the U.S. Department of Energy (Grant No. DE-FG03-94ER14465) for support of this research. Authors L.E.R. and A.S. acknowledge the U. S. Navy Office of Naval Research


 FIG. 11. Fidelity as a function of b .

(Grant No. N00014-03-1-0639) for support of this work. We also acknowledge the University of Texas High Performance Computing Center for use of its facilities.

APPENDIX: CHOOSING $|\Xi_1\rangle$ AND $|\Xi_2\rangle$

To find a unitary matrix that describes the properties of the network of waveguides we start with identifying two 16 component states $|\Xi_1\rangle$ and $|\Xi_2\rangle$ with equal norms that can be constructed out of the elements of Φ_{lft} and Φ_{rt} . It is easy to see how such states may be identified if we assume for the time being that there is no entanglement in the system. This would let us write Φ_{lft} and Φ_{rt} as tensor product of single qutrit states as follows:

$$\begin{aligned} \Phi_{lft} &= (\phi_{l,1}, \phi_{l,2}, \dots, \phi_{l,16}) \\ &= \begin{pmatrix} a_1 \\ a_0 \\ a_u \\ a_d \end{pmatrix} \otimes \begin{pmatrix} b_1 \\ b_0 \\ b_u \\ b_d \end{pmatrix} \\ &= \left[\begin{pmatrix} a_1 \\ a_0 \\ 0 \\ 0 \end{pmatrix} + \begin{pmatrix} 0 \\ 0 \\ a_u \\ a_d \end{pmatrix} \right] \otimes \left[\begin{pmatrix} b_1 \\ b_0 \\ 0 \\ 0 \end{pmatrix} + \begin{pmatrix} 0 \\ 0 \\ b_u \\ b_d \end{pmatrix} \right] \end{aligned} \quad (\text{A1})$$

and

$$\begin{aligned} \Phi_{rt} &= (\phi_{r,1}, \phi_{r,2}, \dots, \phi_{r,16}) \\ &= \begin{pmatrix} e_1 \\ e_0 \\ e_u \\ e_d \end{pmatrix} \otimes \begin{pmatrix} f_1 \\ f_0 \\ f_u \\ f_d \end{pmatrix} \\ &= \left[\begin{pmatrix} e_1 \\ e_0 \\ 0 \\ 0 \end{pmatrix} + \begin{pmatrix} 0 \\ 0 \\ e_u \\ e_d \end{pmatrix} \right] \otimes \left[\begin{pmatrix} f_1 \\ f_0 \\ 0 \\ 0 \end{pmatrix} + \begin{pmatrix} 0 \\ 0 \\ f_u \\ f_d \end{pmatrix} \right]. \end{aligned} \quad (\text{A2})$$

We now rewrite Eqs. (3) and (4) which express the conservation of probabilities in each one of the two qutrits as

$$(|a_1|^2 + |a_0|^2) - (|a_u|^2 + |a_d|^2) = (|e_u|^2 + |e_d|^2) - (|e_1|^2 + |e_0|^2) \quad (\text{A3})$$

and

$$(|f_u|^2 + |f_d|^2) - (|f_1|^2 + |f_0|^2) = (|b_1|^2 + |b_0|^2) - (|b_u|^2 + |b_d|^2). \quad (\text{A4})$$

Dividing Eq. (A3) with Eq. (A4), cross multiplying, and rearranging terms we obtain

$$\begin{aligned}
& (|a_1|^2 + |a_0|^2)(|b_1|^2 + |b_0|^2) + (|a_u|^2 + |a_d|^2)(|b_u|^2 + |b_d|^2) \\
& + (|e_1|^2 + |e_0|^2)(|f_u|^2 + |f_d|^2) + (|e_u|^2 + |e_d|^2)(|f_1|^2 + |f_0|^2) \\
& = (|a_1|^2 + |a_0|^2)(|b_u|^2 + |b_d|^2) + (|a_u|^2 + |a_d|^2)(|b_1|^2 + |b_0|^2) \\
& + (|e_1|^2 + |e_0|^2)(|f_1|^2 + |f_0|^2) + (|e_u|^2 + |e_d|^2)(|f_u|^2 + |f_d|^2).
\end{aligned} \tag{A5}$$

Equation (A5) suggests that the states with coefficients

$$\begin{aligned}
& \begin{pmatrix} a_1 \\ a_0 \\ 0 \\ 0 \end{pmatrix} \otimes \begin{pmatrix} b_1 \\ b_0 \\ 0 \\ 0 \end{pmatrix} + \begin{pmatrix} 0 \\ 0 \\ a_u \\ a_d \end{pmatrix} \\
& \otimes \begin{pmatrix} 0 \\ 0 \\ b_u \\ b_d \end{pmatrix} + \begin{pmatrix} e_1 \\ e_0 \\ 0 \\ 0 \end{pmatrix} \otimes \begin{pmatrix} 0 \\ 0 \\ f_u \\ f_d \end{pmatrix} + \begin{pmatrix} 0 \\ 0 \\ e_u \\ e_d \end{pmatrix} \otimes \begin{pmatrix} f_1 \\ f_0 \\ 0 \\ 0 \end{pmatrix}
\end{aligned} \tag{A6}$$

and

$$\begin{aligned}
& \begin{pmatrix} a_1 \\ a_0 \\ 0 \\ 0 \end{pmatrix} \otimes \begin{pmatrix} 0 \\ 0 \\ b_u \\ b_d \end{pmatrix} + \begin{pmatrix} 0 \\ 0 \\ a_u \\ a_d \end{pmatrix} \\
& \otimes \begin{pmatrix} b_1 \\ b_0 \\ 0 \\ 0 \end{pmatrix} + \begin{pmatrix} e_1 \\ e_0 \\ 0 \\ 0 \end{pmatrix} \otimes \begin{pmatrix} f_1 \\ f_0 \\ 0 \\ 0 \end{pmatrix} + \begin{pmatrix} 0 \\ 0 \\ e_u \\ e_d \end{pmatrix} \otimes \begin{pmatrix} 0 \\ 0 \\ f_u \\ f_d \end{pmatrix}
\end{aligned} \tag{A7}$$

have the same norm. All the coefficients that appear in both these states are elements of Φ_{lft} and Φ_{rt} . Even if there is entanglement in the system the conservation of probability in each quqit is still valid. So, in terms of the elements of Φ_{lft} and Φ_{rt} we can construct the two states Ξ_1 and Ξ_2 which have equal norm and are connected by the unitary matrix U_{QN} through the equation $\Xi_2 = U_{QN} \cdot \Xi_1$.

-
- [1] Radu Ionicioiu, Gehan Amaratunga, and Florin Udrea, *Int. J. Mod. Phys. B* **15**, 125 (2001).
- [2] R. T. Thew, K. Nemoto, A. G. White, and W. J. Munro, *Phys. Rev. A* **66**, 012303 (2002).
- [3] V. M. Kendon, K. Zyczkowski, and W. J. Munro, *Phys. Rev. A* **66**, 062310 (2002).
- [4] K. A. Dennison and W. K. Wootters, *Phys. Rev. A* **65**, 010301 (2001).
- [5] C. E. Shanon, *Bell Syst. Tech. J.* **27**, 379 (1948).
- [6] Rado Ionicioiu, Paolo Zanardi, and Fausto Rossi, *Phys. Rev. A* **63**, 050101 (2001).
- [7] Andrea Bertoni, Rado Ionicioiu, Paolo Zanardi, Fausto Rossi, and Carlo Jacoboni, *Physica B* **314**, 10 (2002).
- [8] C. M. Marcus, A. J. Rimberg, R. M. Westervelt, P. F. Hopkins, and A. C. Gossard, *Phys. Rev. Lett.* **69**, 506 (1992).
- [9] M. A. Eriksson, R. G. Beck, M. Topinka, J. A. Katine, R. M. Westervelt, K. L. Campman, and A. C. Gossard, *Appl. Phys. Lett.* **69**, 671 (1996).
- [10] J. P. Bird, R. Akis, D. K. Ferry, A. P. S. de Moura, Y.-C. Lai, and K. M. Indlekofer, *Rep. Prog. Phys.* **66**, 1 (2003).
- [11] S. Datta, *Electronic Transport in Mesoscopic Systems* (Cambridge University Press, Cambridge, 1995).
- [12] M. A. Nielsen and I. L. Chuang, *Quantum Computation and Quantum Information* (Cambridge University Press, Cambridge, 2000).
- [13] A. Bertoni, P. Bordone, R. Brunetti, C. Jacoboni, and S. Reggiani, *Phys. Rev. Lett.* **84**, 5912 (2000).
- [14] J. Harris, R. Akis, and D. K. Ferry, *Appl. Phys. Lett.* **79**, 2214 (2001).
- [15] M. J. Gilbert, R. Akis, and D. K. Ferry, *Appl. Phys. Lett.* **81**, 4284 (2002).
- [16] M. J. Gilbert, R. Akis, and D. K. Ferry, *Appl. Phys. Lett.* **83**, 1453 (2003).
- [17] G. B. Akguc and L. E. Reichl, *J. Stat. Phys.* **98**, 813 (2000).
- [18] G. B. Akguc and L. E. Reichl, *Phys. Rev. E* **64**, 056221 (2001).
- [19] G. B. Akguc and L. E. Reichl, *Phys. Rev. E* **67**, 046202 (2003).
- [20] Masahiro Kitagawa and Masahito Ueda, *Phys. Rev. Lett.* **67**, 1852 (1991).